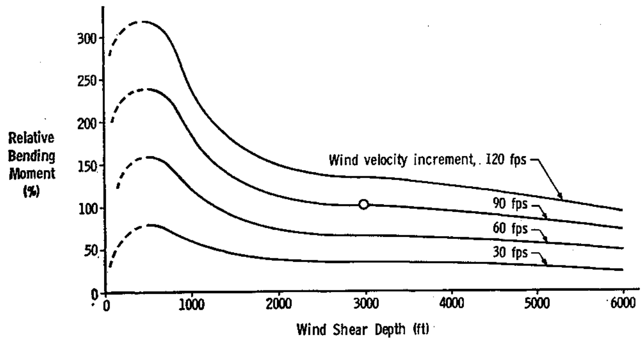

Fig. 6 Variation of relative bending moment with shear depth for constant wind velocity

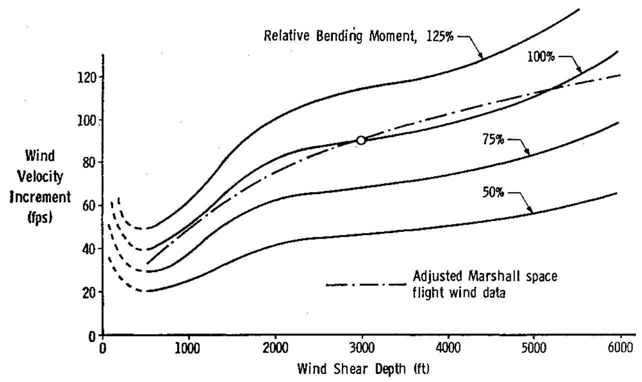

Fig. 7 Variation of wind velocity with shear depth for constant relative bending moment

ft was selected as the 100% level. The effects of the characteristics of an arbitrary wind shear reversal can be assessed from these data. Changes in wind velocity increment or shear depth can be expressed in terms of an increase or decrease in bending moment. The combinations of wind velocity increment and shear depth that produce the same relative bending moment level are presented in Fig. 7.

The wind velocity increments associated with shear depths other than 3000 ft have been determined for the 10- to 14-km region.[3] Normalizing the magnitudes of these velocity increments about the 3000-ft value will give the variation of wind velocity for depths other than 3000 ft. The dotted portion of the data in Fig. 7 is based on these adjusted variations of velocity increment with shear depth, the basis being an increment of 90 fps over a depth of 3000 ft.

Comparison of the adjusted data of Fig. 7 with 100% load level indicates that the 3000-ft shear depth does not produce critical loading. The critical depth lies between 3000 and 5200 ft, at approximately 4000 ft, which corresponds to a relative bending moment of about 105%.

The study illustrates that the maximum loading occurred at a depth in excess of 3000 ft, which demonstrates that wind criteria established to produce a given risk in terms of structural capability are vulnerable to changes in configuration, flight control system, etc. However, it does show that such criteria are adequate in the design of R&D boosters, since launch dates can be selected.

References

[1] Hobbs, N. P., Criscione, E. S., Mazzola, L. L., and Frassinelli, G. J., "Development of interim wind shear and gust design criteria for vertically rising vehicles" (unclassified title), Wright Air Dev. Center TR 59-504, AviDyne Research Inc. (July 1959).

[2] Easley, J. W. and Walkenhorst, W. F., "Approach to development of comprehensive wind design criteria," *Proceedings of the National Symposium on Winds for Aerospace Vehicle Design* (Geophys. Res. Dir., Air Force Cambridge Res. Labs., L. G. Hanscom Field, Bedford, Mass., 1962), Vol. 2, no. 140, pp. 103–118.

[3] Scoggins, J. R. and Vaughan, W. W., "Cape Canaveral wind and shear data (1 through 80 km) for use in vehicle design and performance studies," NASA TN D1274 (July 1962).

Rarefied-Gas Field Equations for Plane Shear Disturbance Propagation

J. G. Logan*
Aerospace Corporation, Los Angeles, Calif.

In a recent note,[1] the two-dimensional linearized Grad equations for the rarefied-gas field, when applied to the Rayleigh problem, were shown to yield the following characteristic equations for the propagation of small shear disturbances:

$$\left[\frac{\partial}{\partial t} \pm \left(\frac{7}{5}\right)^{1/2} \frac{\partial}{\partial y}\right] Q_{\pm}(y, t) = -\frac{L}{t_f c_0}\left[\frac{P_{xy}}{p_0} \pm \frac{4}{3(35)^{1/2}} \frac{q_x}{p_0 c_0}\right] \quad (1)$$

where the propagating quantity Q is given by

$$Q_{\pm} = \left[\frac{P_{xy}}{p_0} \pm \left(\frac{u}{c_1} + \frac{2}{5}\frac{q_x}{p_0 c_1}\right)\right]$$

P_{xy} is the shear stress, u the disturbance velocity, q_x the heat flux, c_1 the propagation velocity defined by

$$c_1 = (\tfrac{7}{5})^{1/2} c_0 = (\tfrac{7}{5} R T_0)^{1/2} \qquad c = c_1/c_0$$

p_0 is the equilibrium pressure and T_0 the equilibrium temperature. The relaxation time is defined by $t_f \simeq \mu_0/p_0$, i.e., the ratio of viscosity to pressure.

In the limit $t_f \gg L/c_0$, Eq. (1) can be written as

$$[(\partial/\partial t) \pm c(\partial/\partial y)]Q_{\pm} = 0 \quad (2)$$

Consequently, in the limit of large relaxation time, plane shear disturbances initiated by field particle collisions with a boundary will propagate unchanged through the field.

As an illustrative example, the disturbance produced by the impulsive motion of an infinite plate in a rarefied-gas field, initially in equilibrium at a temperature T_0, can be calculated assuming that specular reflection does not occur at the boundary (Fig. 1). The field particles are absorbed and reemitted with a Maxwellian distribution at the temperature T_0 and the shear velocity U. Hence,

$$Q_+ = \frac{P_{xy}}{p_0} + \frac{u}{c_1} + \frac{2}{5}\frac{q_x}{p_0 c_1} = \frac{U}{c_1} \qquad P_{xy} = q_x = 0$$

The complimentary characteristic quantities for the small longitudinal disturbances[1] yield $P_{1+} = P_{2+} = 0$, where

$$P_{1+} = \theta - 0.51p - 0.11\frac{P_{yy}}{p_0} + 0.33\frac{q_y}{p_0 c_0} - 0.42\frac{v}{c_0}$$

$$P_{2+} = \theta + 0.78p + 1.18\frac{P_{yy}}{p_0} + 0.85\frac{q_y}{p_0 c_0} + 1.66\frac{v}{c_0}$$

When the disturbance Q reaches boundary (B), Fig. 1, the following mass, momentum, and energy conditions must be satisfied:[2]

$$p + \tfrac{1}{2}(P_{yy}/p_0) = s_w \quad (3)$$

$$\frac{P_{xy}}{p_0} + 0.16\frac{q_x}{p_0 c_0} = 0.8\frac{U}{c_0} + 0.4\frac{P_{yy}}{p_0}\frac{U}{c_0} \approx 0.8\frac{U}{c_0} \quad (4)$$

$$(P_{yy}/p_0) + 2.51(q_y/p_0 c_0) = (U/c_0)^2 \quad (5)$$

on assuming a wall condition such that $\theta = \theta_w = 0$ and $u = 0$.

Received by IAS November 26, 1962; revision received January 2, 1963.

* Director, Aerodynamics and Propulsion Research Laboratory. Member AIAA.

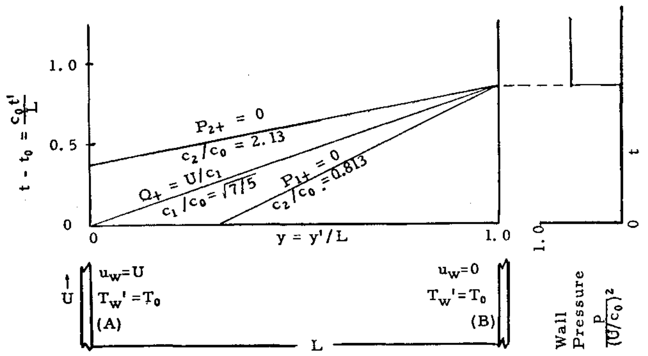

Fig. 1 Characteristic diagram for plane shear disturbance propagation

The boundary conditions and characteristic equations $P_{1+} = P_{2+} = 0$, $\perp Q_+ = U/c_1$ yield

$$\frac{q_y}{p_0c_0} = 0.86\left(\frac{U}{c_0}\right)^2 \quad \frac{P_{yy}}{p_0} = -1.15\left(\frac{U}{c_0}\right)^2 \quad p = 0.80\left(\frac{U}{c_0}\right)^2$$

$$\frac{q_x}{p_0c_0} = 0.27\,\frac{U}{c_0} \quad \frac{P_{xy}}{p_0} = 0.76\,\frac{U}{c_0} \quad s_w = 0.23\left(\frac{U}{c_0}\right)^2$$

The second-order coupling, through the energy equation, between the longitudinal and transverse disturbances at the boundary results, for this idealized example, in a pressure or normal force at the boundary proportional to $(Q_+)^2$. The shear wave consequently transmits momentum and energy and produces a pressure at the wall proportional to the square of the amplitude of the disturbance Q. The behavior is analogous to that of a plane electromagnetic wave.

If $\mathbf{n}_y$ is defined as a unit vector along the y direction, the direction of propagation, Eq. (2) for the forward propagation of a plane, rarefied-gas shear disturbance, in vector notation, may be written in the form ($\mathbf{n}_y = \mathbf{j}$)

$$[\mathbf{j}(1/c)(\partial/\partial t) + \nabla]\times\mathbf{Q}_1 = 0 \tag{6}$$

$$\left(\mathbf{j}\,\frac{1}{c}\,\frac{\partial}{\partial t} + \nabla\right)\cdot\mathbf{Q}_1 = 0 \qquad [\mathbf{Q}_1 = \mathbf{i}Q_x(y,t)] \tag{7}$$

Equations (6) and (7) may be written in the alternate form

$$\nabla\times\mathbf{Q}_1 + (1/c)(\partial/\partial t)(\mathbf{j}\times\mathbf{Q}_1) = 0 \tag{6'}$$

$$\nabla\cdot\mathbf{Q}_1 = 0 \qquad \mathbf{j}\cdot\mathbf{Q}_1 = 0 \tag{7'}$$

Independent shear disturbances also can be generated in the z direction which will simultaneously propagate in the y direction and satisfy

$$\left(\mathbf{j}\,\frac{1}{c}\,\frac{\partial}{\partial t} + \nabla\right)\times\mathbf{Q}_2 = 0 \quad \text{or} \quad \Delta\times\mathbf{Q}_2 + \frac{1}{c}\,\frac{\partial}{\partial t}\,(\mathbf{j}\times\mathbf{Q}_2) = 0 \tag{8}$$

$$\left(\mathbf{j}\,\frac{1}{c}\,\frac{\partial}{\partial t} + \nabla\right)\cdot\mathbf{Q}_2 = 0 \quad \text{or} \quad \nabla\cdot\mathbf{Q}_2 = \mathbf{j}\cdot\mathbf{Q}_2 = 0$$

where $\mathbf{Q}_2 = -\mathbf{k}Q_z(y,t)$. Hence, the shear disturbances for the Rayleigh problem satisfy the equations

$$\nabla\times\mathbf{Q}_1 + (1/c)(\partial/\partial t)(\mathbf{j}\times\mathbf{Q}_1) = 0 \tag{9}$$

$$\nabla\times\mathbf{Q}_2 + (1/c)(\partial/\partial t)(\mathbf{j}\times\mathbf{Q}_2) = 0 \tag{10}$$

$$\nabla\cdot\mathbf{Q}_1 = 0 \tag{11}$$

$$\nabla\cdot\mathbf{Q}_2 = 0 \tag{12}$$

For the special case of equal-amplitude impulsive motions in the x and z directions, for which $Q_x = Q_z$, $\mathbf{j}\times\mathbf{Q}_1 = \mathbf{Q}_2$, and $\mathbf{j}\times\mathbf{Q}_2 = -\mathbf{Q}_1$. Equations (9–11) may, consequently, be written in the alternate form[3]

$$\nabla\times\mathbf{Q}_1 + (1/c)(\partial/\partial t)\mathbf{Q}_2 = 0 \tag{13}$$

$$\nabla\times\mathbf{Q}_2 - (1/c)(\partial/\partial t)\mathbf{Q}_1 = 0 \tag{14}$$

$$\nabla\cdot\mathbf{Q}_1 = \nabla\cdot\mathbf{Q}_2 = 0 \tag{15}$$

The characteristic equations for the propagation of small, equal-amplitude, plane, shear disturbances in a rarefied-gas field satisfy equations identical in form with the Maxwell equations for the propagation of plane electromagnetic disturbances in a vacuum. These equations are[4]

$$\nabla\times\mathbf{E} + (1/c)(\partial\mathbf{H}/\partial t) = 0 \tag{16}$$

$$\nabla\times\mathbf{H} - (1/c)(\partial\mathbf{E}/\partial t) = 0 \tag{17}$$

$$\nabla\cdot\mathbf{H} = \nabla\cdot\mathbf{E} = 0 \tag{18}$$

where $\mathbf{E}$ is the electric field, $\mathbf{H}$ the magnetic field, and c the propagation velocity. This similarity immediately suggests the possibility of interpreting the Maxwell equations as characteristic equations describing the propagation of small shear disturbances in the vacuum electromagnetic field.

For the special case of a plane electromagnetic wave with an electric field $\mathbf{E} = \mathbf{i}E_x(y,t)$ propagating in a forward direction along the y axis, the Maxwell equations yield,[4] for $\mathbf{H} = \mathbf{k}H_z(y,t)$,

$$\mathbf{H} = \mathbf{k}H_z(y,t) = \mathbf{j}\times\mathbf{E} = \mathbf{j}\times\mathbf{i}E_x(y,t) = -\mathbf{k}E_x(y,t)$$

or

$$H_z(y,t) = -E_x(y,t)$$

The Maxwell equations (16) and (17) may be written in the form

$$\nabla\times\mathbf{E} + (1/c)(\partial/\partial t)(\mathbf{j}\times\mathbf{E}) = 0 \tag{19}$$

$$\nabla\times\mathbf{H} + (1/c)(\partial/\partial t)(\mathbf{j}\times\mathbf{H}) = 0 \tag{20}$$

Hence, Eqs. (19) and (20) state that, for plane wave propagation, the electric and magnetic fields satisfy the characteristic equations

$$[(\mathbf{j}/c)(\partial/\partial t) + \nabla]\times\mathbf{E} = 0 \tag{21}$$

$$[(\mathbf{j}/c)(\partial/\partial t) + \nabla]\times\mathbf{H} = 0 \tag{22}$$

The Maxwell equations do not, however, include the time-dependent equation for the propagation of small plane longitudinal disturbances. If, in analogy with the equations describing the propagation of small plane longitudinal disturbances in rarefied gas fields,[5]

$$[(\mathbf{j}/c_1)(\partial/\partial t) + \nabla]\times\mathbf{P} = 0 \tag{23}$$

$$[(\mathbf{j}/c_1)(\partial/\partial t) + \nabla]\cdot\mathbf{P} = 0 \qquad \mathbf{P} = \mathbf{j}P(y,t) \tag{24}$$

parallel equations are defined for this longitudinal propagation along the y axis, viz.,

$$[(\mathbf{j}/c)(\partial/\partial t) + \nabla]\times\mathbf{E} = 0 \qquad \mathbf{E} = \mathbf{j}E_y(y,t) \tag{25}$$

$$[(\mathbf{j}/c)(\partial/\partial t) + \nabla]\cdot\mathbf{E} = 0 \tag{26}$$

the longitudinal disturbances satisfy

$$\nabla\times\mathbf{E} = 0 \tag{27}$$

$$\nabla\cdot\mathbf{E} + (1/c)(\partial/\partial t)(\mathbf{j}\cdot\mathbf{E}) = 0 \tag{28}$$

Similar equations can be written for $\mathbf{H}$. Equation (28) would enable a description of the nonsteady propagation of small plane longitudinal disturbances, associated with static electric fields, which also must exist in the vacuum field and propagate with a velocity c.

References

[1] Logan, J. G., "A further note on propagation of transverse disturbances in rarefied-gas flows," AIAA J. 1, 943–945 (1963).

[2] Yang, H. and Lees, L., "Rayleigh's problem at low Mach number according to the kinetic theory of gases," J. Math. Phys. 35, 195–235 (October 1956).

[3] Logan, J. G., "Hydrodynamic analog of the classical field equations," Phys. Fluids **5**, 868–869 (1962).

[4] Landau, L. and Lifshitz, E., *The Classical Theory of Fields* (Addison-Wesley Press Inc., Cambridge, Mass., 1951), pp. 114–117.

[5] Logan, J. G., "A further note on propagation of thermal disturbances in rarefied-gas flows," AIAA J. **1**, 942–943 (1963).

Residual Tensile Strength of Cracked Structural Elements

George Gerard*
Allied Research Associates, Concord, Mass.

Nomenclature

a = finite width correction factor
d = ligament width, in.
e = ductility ratio
k_e = elastic stress-concentration factor
k_p = plastic stress-concentration factor
k_s = stress-concentration strengthening factor
k_∞ = elastic stress-concentration factor for infinite width
L = notch length, in.
r = notch or crack radius, in.
w = width, in.
σ_{tu} = ultimate tensile strength, ksi
σ_{ty} = tensile yield strength, ksi

Introduction

An analytical procedure for predicting the effects of determinate stress-concentration factors upon the strength of structural elements has been presented in Ref. 1. This method is based upon the reference value of the elastic stress-concentration factor in the structural element (which generally depends upon the local radius of curvature) and a characteristic of the material called the ductility ratio.

The limiting case of a stress concentration in a structural element is a crack. Here, the stress-concentration factor is indeterminate since the local radius of curvature is some function of the microstructure of the material and cannot be evaluated readily. Since the residual tensile strength of a structure containing relatively small cracks is of vital interest in many aerospace vehicle applications, it is of considerable importance to devise phenomenological approaches to this problem.

In the following, a modified stress-concentration factor approach is presented for determining the residual strength of structural elements containing cracks of limited extent. The ductility ratio that characterizes the material in the presence of a stress concentration and the effective radius of the crack are evaluated as a single material parameter from the test data correlation scheme presented herein.

Stress Concentration Factor Approach

Elastic stress concentration factors

For an infinitely wide sheet containing a central slit normal to the applied tension, Inglis[2] derived the following relation for the elastic stress-concentration factor in terms of the radius at the end of the slit r and the slit half-length L (see Fig. 1):

$$k_\infty = 1 + 2\,(L/r)^{1/2} \tag{1}$$

In an extension of Inglis' result to strips of finite width, Dixon[3] derived the following correction factor:

$$a = \frac{k_e}{k_\infty} = \left(\frac{d/w}{2 - d/w}\right)^{1/2} \tag{2}$$

By combining Eqs. (1) and (2),

$$k_e = a\,[1 + 2\,(L/r)^{1/2}] \tag{3}$$

Both Eqs. (2) and (3) have been confirmed by photoelastic test results reported by Dixon[3] and Papirno.[4] For convenience, the finite width correction factor given by Eq. (2) is plotted in Fig. 1.

Plastic stress concentration factors

Equations (1–3) pertain to the elastic region of the stress-strain curve of a material. In the plastic region and at failure, it is necessary to consider the influence of plasticity upon the elastic stress-concentration factor. In Ref. 1, the following semi-empirical relationship between the plastic stress-concentration factor k_p and the elastic one was suggested:

$$k_p = (1/k_s) + [k_e - (1/k_s)]e \tag{4}$$

Here, e is the ductility ratio that is a characteristic of the material. The factor k_s accounts for the notch strengthening resulting from the multiaxial stress field existing in the vicinity of the notch.

By rearranging Eq. (4) in the following form,

$$k_p = (1/k_s)(1 - e) + k_e e \tag{5}$$

it is possible to evaluate both e and k_s from a series of strength tests on specimens containing determinate stress-concentration factors in which the net section stress is elastic. This procedure is illustrated in some detail in Refs. 1 and 5 and consists of plotting k_p vs k_e, which generally is linear. The ductility ratio then is evaluated from the slope and k_s from the intercept.

Now, by inserting Eq. (3) into Eq. (5), one obtains

$$k_p = (1/k_s)(1 - e) + ae + 2\,a\,L^{1/2}\,(e/r^{1/2}) \tag{6}$$

In cases where the slit length is held fixed and r is varied to achieve different determinate stress-concentration factors, then L, a, and k_s are fixed quantities. By plotting k_p vs $r^{1/2}$, when the net section stress is elastic, the ductility ratio can be evaluated from the slope of the straight line and k_s from the intercept. This procedure corresponds essentially to that used in connection with Eq. (5).

Indeterminate stress concentrations

When cracks are considered, however, the geometric conditions of the problem are somewhat different. Now, the radius at the root of the crack is essentially constant, although

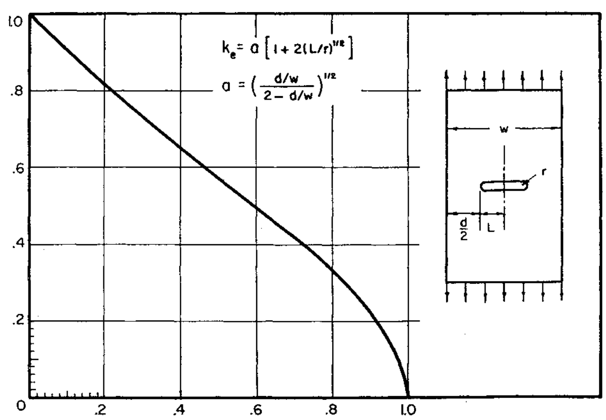

Fig. 1 Elastic stress concentration for an internally notched tension strip of finite width

Received by IAS November 29, 1962.

* Director of Engineering Sciences. Associate Fellow Member AIAA.